Tikrit Journal of Pharmaceutical Sciences 2023; 17(1):58-77
http://doi.org/10.25130/tjphs.2023.17.1.6.58.77

IRAQI Academic Scientific Journals

Tikrit Journal of Pharmaceutical Sciences

Available online at: https://tjphs.tu.edu.iq

ISSN: 1815-2716(print); ISSN: 2664-231X (online)

T. J. Ph. S.

Synthesis and docking studies of new 5-bromoindole-2-carboxylic acid oxadiazole derivatives as EGFR inhibitors

Omeed Muhsin Hassan[1*], Ammar A. Razzak Mahmood[2], Lubna Tahtamouni[3,4]

1.Department of Pharmaceutical Chemistry, College of Pharmacy, University of Kirkuk. Kirkuk -Iraq.

2. Department of Pharmaceutical Chemistry, College of Pharmacy, Bab-Al-Mouadam,10001. University of Baghdad Bagdad-Iraq

3Department of Biology and Biotechnology, Faculty of Science, The Hashemite University, Zarqa, Jordan.

4Department of Biochemistry and Molecular Biology, College of Natural Sciences, Colorado State University, Fort Collins, Colorado, USA..

ARTICLE INFO.

Article history:

-Received: 12/02/2023

-Accepted: 10/03/2023

-Available online: 23/ 06/2023

Keywords:

Indole, Oxadiazole, Docking studies, DFT, EGFR receptor tyrosine kinase.

***Corresponding author:**

Omeed Mohsin Hassan

Email : omeedtarzi@yahoo.com

Contact To Journal

E-mail: tjops@tu.edu.iq

Citation:

Hassan O. M., Mahmood A. A., Tahtamouni L. Synthesis and docking studies of new 5-bromoindole-2-carboxylic acid oxadiazole derivatives as EGFR inhibitors. Tikrit Journal of Pharmaceutical Sciences 2023; 17(1):58-77.
http://doi.org/10.25130/tjphs.2023.17.1.6.58.77

Abstract

The current study reports the design and synthesis of novel oxadiazole derivatives of 5-bromoindole-2-carboxylic acid and their molecular docking properties. In order to determine the structure of the new oxadiazole derivatives (3, 4a, 4b), a number of spectroscopic techniques (IR and ^{1}HNMR) were employed. Molecular docking analysis indicated that compounds 3, 4a, 4b showed favorable binding free energy against the EGFR tyrosine kinase domain. None of these compounds appeared to suppress cytochrome P450, and all of them showed appropriate absorption levels. Moreover, they did not exhibit any hepatotoxicity when tested *in vitro*. Compound 4a Reported to have the highest stability, with a good net binding energy, and an excellent binding energy with hot amino acids. Dipole moment is also rather high. This result is an indication of compound 4a is with superior capacity to create hydrogen bonds over erlotinib. Likewise, compound 4a was found to be the most stable in its interaction with EGFR tyrosine kinase. Finally, molecular dynamic simulation revealed excellent outcomes for compound 4a.

تخليق ودراسة الرسو لمشتقات الاوكسادايزول الجديدة مشتقة من ٥-برومو-٢ اندول حامض كاربوكسيلي كمثبطات لمستقبلات عامل النمو البطاني الوعائي

الخلاصة

تشير الدراسة الحالية إلى تصميم وتوليف مشتقات أوكساديازول الجديدة لحمض ٥-:بروموانـدول -٢-كربوكسيليك وخصائصها الجزيئية. من أجل تحديد بنية مشتقات أوكساديازول الجديدة (٣ ، ٤ أ ، ٤ ب) ، تم استخدام عدد من التقنيات الطيفية (IR و HNMR1). أشار تحليل الالتحام الجزيئي إلى أن المركبات ٣ ، ٤ أ ، ٤ ب أظهرت طاقة ارتباط حرة مواتية ضد مستقبلات EGFR التيروزين كيناز. لا يبدو أن أيًا من هذه المركبات يقمع السيتوكروم P450 ، وأظهرت جميعها مستويات امتصاص مناسبة. علاوة على ذلك ، لم تظهر عليهم أي سمية كبدية عند اختبارها في المختبر. تم الاشارة الى أن المركب ٤ أ يتمتع بأعلى مستوى من الاستقرار ، مع طاقة ارتباط شبكية جيدة ، وطاقة ارتباط ممتازة مع الأحماض الأمينية الساخنة. العزم ثنائي القطب مرتفع أيضًا. هذه النتيجة هي إشارة إلى أن المركب ٤ أ يتمتع بقدرة فائقة على تكوين روابط هيدروجينية تفوق الارلوتنيب. وبالمثل ، وجد أن المركب ٤ أ هو الأكثر استقرارًا في تفاعله مع EGFR التيروزين كيناز. أخيرًا ، كشفت المحاكاة الديناميكية الجزيئية عن نتائج ممتازة للمركب ٤ أ.

Introduction

Cancer is a complex disorder characterized by abnormal cell growth that evades the body's normal regulating mechanisms. [1] Cancer is the world's second leading cause of death and is widely regarded as one of the worst diseases ever. [2] As a result, scientists have developed a number of promising new cancer treatments, and a wide range of chemicals have been approved for use. Because indole has promising anti-cytotoxic effects by targeting a wide range of proteins and enzymes, synthetic indole derivatives and associated signaling pathways have been studied. [3] Indole's potential as a cytotoxic agent is highlighted by the ability of the nitrogen atom to establish hydrogen bonds with the targets. The success of indole-based cytotoxic agents such as vincristine has inspired the development of improved cytotoxic indole derivatives. [4]

The epidermal growth factor receptor, or EGFR, is a transmembrane glycoprotein with a single polypeptide chain of 1186 amino acids. [5] Autophosphorylation of certain tyrosine residues occur upon receptor dimerization in response to growth factor binding. When the EGFR tyrosine kinase domain is active, SOS, a Ras GDP/GTP exchange factor, is recruited to attach to the activated EGFR on the inside of the cell. As a result, signal transduction cascades such as the Ras-MAP kinase pathway is activated, which triggers DNA synthesis, cell division, and differentiation. [6] Cell cycle transition from G1 to S phase can also be affected by EGFR tyrosine kinase activity. [7] EGFR overexpression has been linked to a variety of cancer types, and as a result, EGFR inhibition has been studied. Anti-EGFR monoclonal antibodies such as panitumumab, which are competitive inhibitors of EGFR ligand binding, and EGFR tyrosine kinase inhibitors such as erlotinib, which are small molecules that inhibit EGFR intracellular tyrosine kinase, are currently used to inhibit EGFR. [8] Some forms of cancer can now be treated successfully with these methods. Unfortunately, even when these therapies are used, resistance is still a common phenomenon. Two major sources of resistance are the T790M mutation and the MET oncogene. [9]

As a result, scientists have been hard at work developing new anti EGFR treatments. Oxadiazole is a heterocyclic molecule containing two nitrogen atoms and one oxygen atom forming a five-membered structure with the chemical formula $C_2H_2N_2O$. [10] Numerous oxadiazole derivatives have been synthesized with pharmaceutical uses such

as 1,2,4-oxadiazole, 1,2,5-oxadiazole, and 1,3,4-oxadiazole. [11] Zibotentan, N-(3-methoxy-5-methylpyrazin-2-yl)-2-[4-(1,3,4-oxadiazol-2-yl)phenyl]pyridine-3-sulfonamide, has been shown to inhibit cell proliferation and stimulate apoptosis of tumor cells. The current study was carried out to synthesize novel oxadiazole derivatives of 5-bromoindole-2-carboxylic acid and to evaluate their EGFR receptor tyrosine kinase inhibition in silico.

Experimental

Materials and Methods

Chemicals and solvents were purchased from (HyperChem, China), and used without any additional purification. An Attenuated Total Reflection Fourier Transform Infrared (ATR-FTIR, ύ = cm^{-1}) spectrophotometer (Shimadzu GS 10800/R IR- Affinity) was used to obtain infrared spectrum. Using a 300MHz AVANCE-III Nano-bay FT-NMR spectrometer, we recorded the ^{1}HNMR spectra of the synthesized compounds, respectively. The chemical shift was reported in ppm units, tetramethyl silane (TMS) served as the internal standard, and $DMSO_{d6}$ was used as the solvent. Verifying the progress of the reactions was accomplished by TLC, using different ratios of solvents (60% hexane: 40%EtOAc) and (50% acetone: 50% petroleum ether).

Chemical Synthesis

Synthesis of ethyl 5-bromo-1*H*-indole-2-carboxylate (compound 1)

The synthesis protocol was carried out according to previously published work. [12]

Synthesis of 5-bromo-1*H*-indole-2-carbohydrazide (compound 2)

The synthesis protocol was carried out according to previously published work. [13]

Synthesis of 5-(5-bromo-1*H*-indol-2-yl)-1,3,4- oxadiazole-2(3*H*)-thione (Compound 3) [14]

In 100 ml round bottom flask A mixture of compound (**2**) (1.27 g, 0.005 mol) and carbon disulfide (CS_2),(0.015 mol, 1.5 mL) in the presence of alcoholic potassium hydroxide (0.45 g, 0.008 mol) in ethanol (35 mL) was refluxed for 15 h. The product mixture was cooled and acidified to pH 3-4 with diluted hydrochloric acid (HCl) solution and re-crystallized from 60% ethanol.

Light gray powder, yield (72%), m.p = (257-259 ^{0}C), R_f.= 0.54 ATR-FTIR (ύ, cm^{-1}): 3197.98 (NH) str. indole, 2642.48 (SH) str. of oxadiazole, 1631.78 (C=C) str, 1531.48 (C=N) str., 1327.03 (C-N) str. ,1161.15,1083.99 (C-O-C) str, 794.67 (aromatic di- substitution), 705.95 (C-Br) str. (Figure 1).^{1}HNMR (300 MHz, $DMSO_{d6}$, δ=ppm): 12.4 (s,1H,NH-thione),

7.9 (d,1H,Ar-H), 7.4-7.1 (m,3H,ArH) (Figure 2).

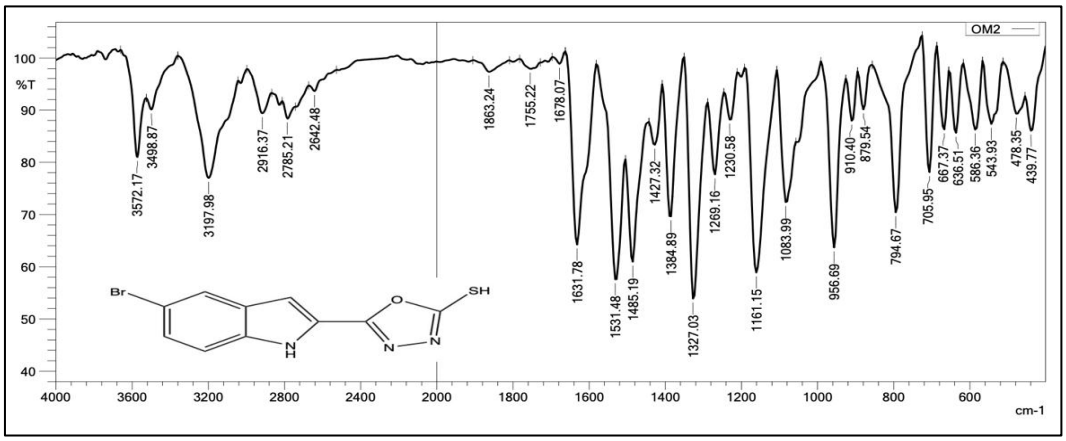

Figure 1. Infrared spectrum of compound 3.

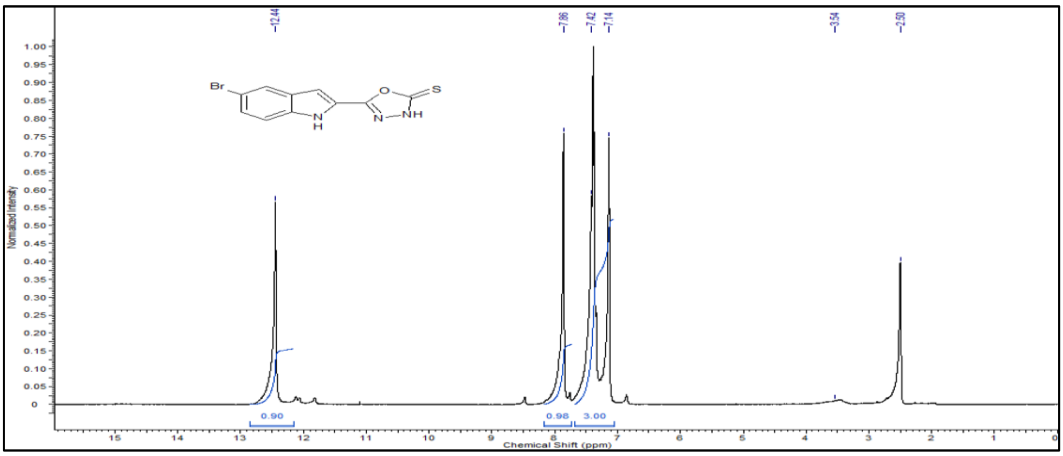

Figure 2. ^{1}HNMR spectrum of compound 3.

Method of synthesis of 1,3,4-oxadiazole derivatives

A mixture of compound **3** (0.5 g, 0.0017 mol) with few drops of triethyl amine were stirred in ethanol (30 mL) for 5 min, and then an equimolar amount of an appropriate phenacyl bromide: 2-Bromo-4-bromoacetophenone, 2-Bromo-4-chloroacetophenone (0.0017 mol) were added separately and slowly and stirred at room temperature for 4 hours. The collected product was washed with D.W and dried then crystallized from ethanol/DMF.

Synthesis of 2- ((5- (5-bromo- 1H- indol -2 -yl) -1,3,4 – oxadiazol -2- yl) thio) -1- (4-bromophenyl) ethan-1-one (Compound 4a)

Sand color powder, yield (66%), m.p = (277-280 ^{0}C), R_f.= 0.6 ATR-FTIR (ύ, cm^{-1}): 3209.55 (NH) str. indole, 1674.21 (C=O) str, 1620.21 (C=C) str., 1577.77 (C=N) str.,1165.00,1064.71 (C-O-C) str, 802.39 (aromatic di-substitution), 721.38 (C-Br) str. (Figure 3).

^{1}HNMR (300 MHz, DMSO$_{d6}$, δ=ppm): 12.5 (s,1H,NH-indole), 8.0-7.8

(m,5H,Ar-H), 7.4-7.1 (m,3H,ArH), 5.2 (s, 2H,S-$\underline{CH_2}$-C=O) (Figure 4)

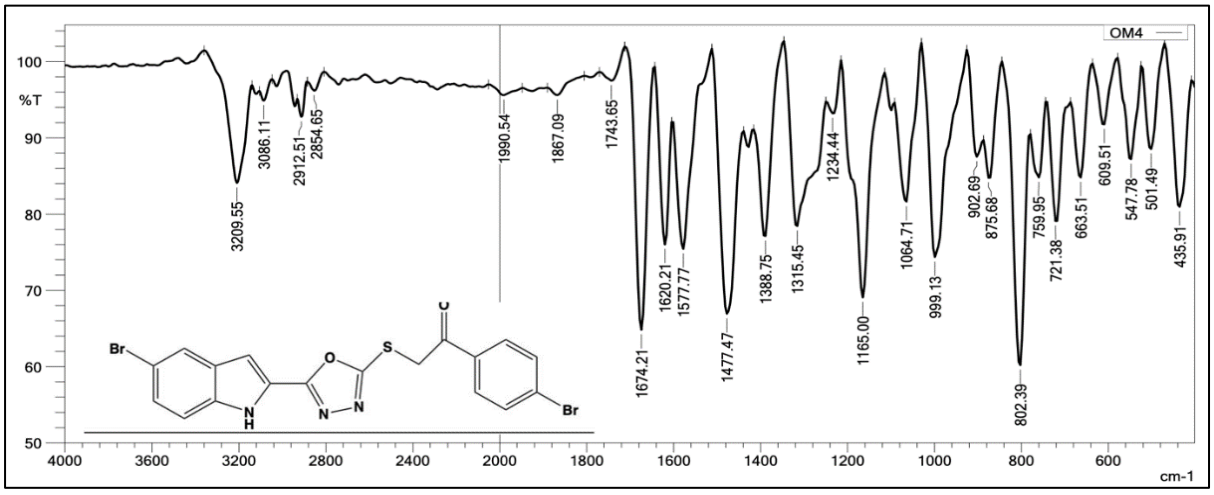

Figure 3. Infrared spectrum of compound 4a.

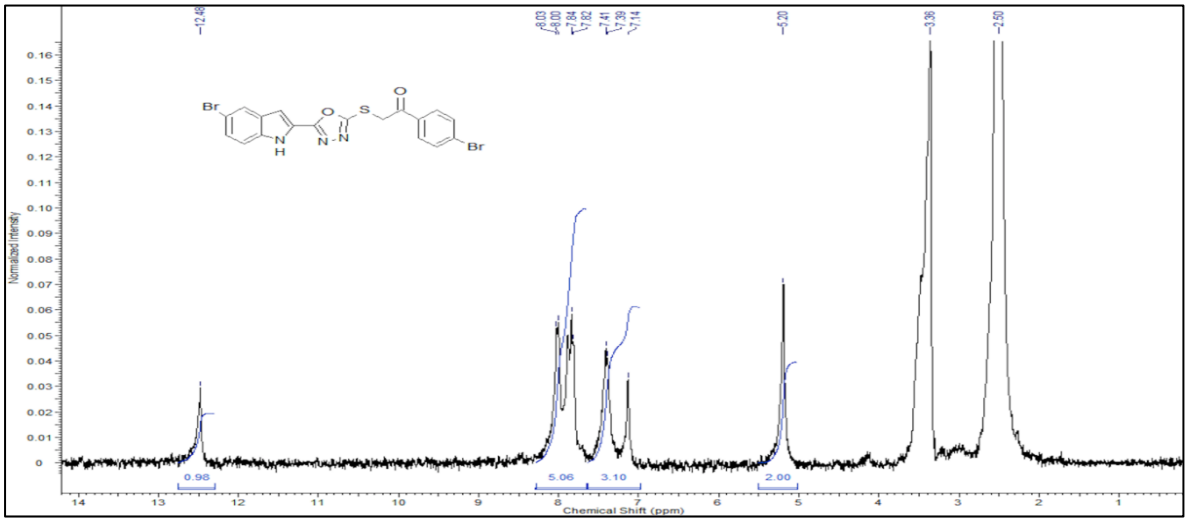

Figure 4. ^{1}HNMR spectrum of compound 4a.

Synthesis of 2- ((5- (5-Bromo- 1*H*-indol-2-yl) -1,3,4- oxadiazol -2-yl) thio) -1- (4-chlorophenyl) ethan-1-one (Compound 4b)

White color powder, yield (77%), m.p = (269-272 ^{0}C), R_f= 0.63 ATR-FTIR (ύ, cm^{-1}): 3205.69 (NH) str. indole, 1678.07 (C=O) str, 1620.21 (C=C) str, 1589.34 (C=N) str,1165.00,1091.71 (C-O-C) str, 806.25 (aromatic di-substitution), 721.38 (C-Br) str. (Figure 5).

^{1}HNMR (300 MHz, DMSO$_{d6}$, δ=ppm): 12.5 (s,1H,NH-indole) , 8.1 (d,2H,Ar-H), 7.9 (s,1H,ArH), (7.68) (d, 2H,Ar-H), (7.41) (dd,2H,Ar-H), 7.1(s,1H,Ar-H), 5.2 (s, 2H,S-$\underline{CH_2}$-C=O) (Figure 6).

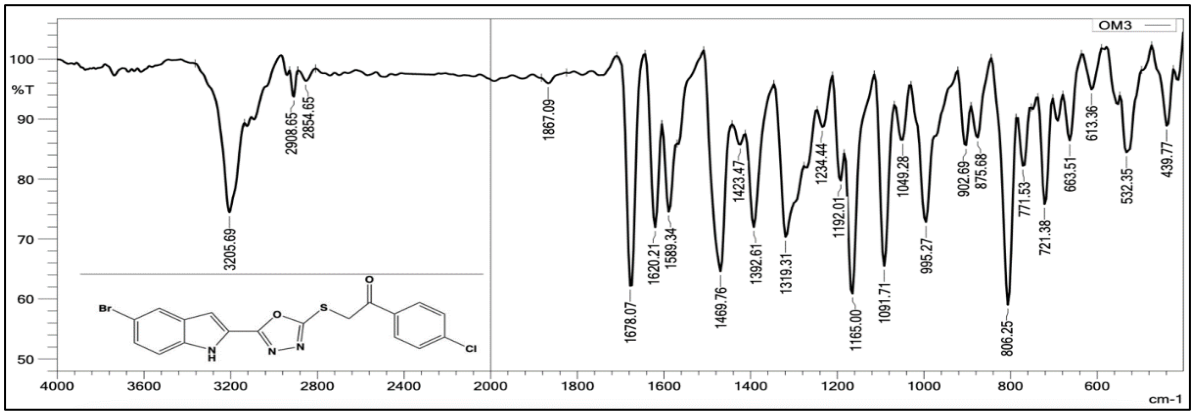

Figure 5. Infrared spectrum of compound 4b.

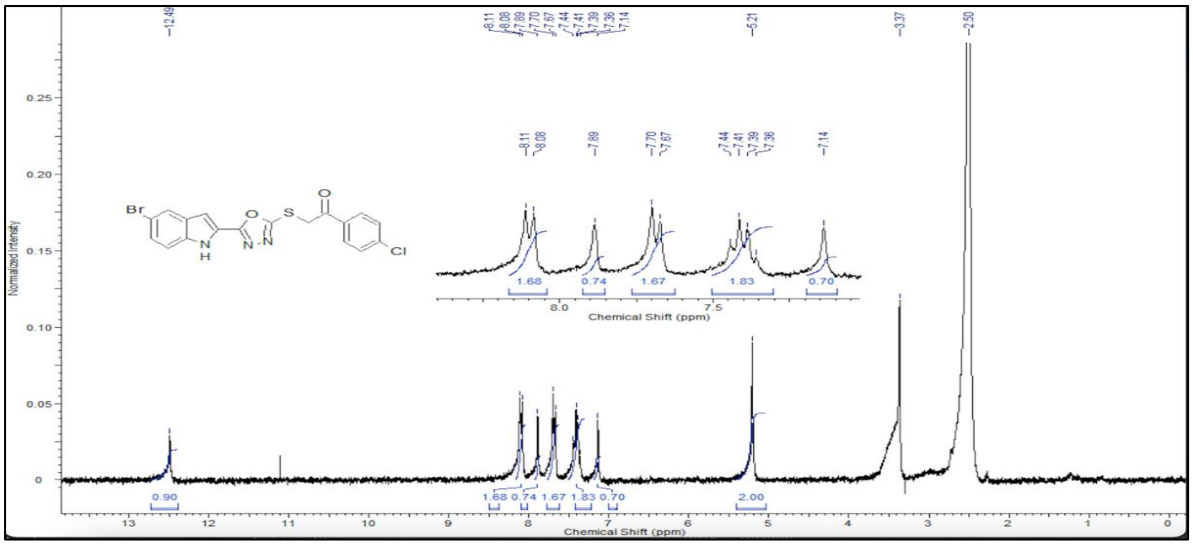

Figure 6. ^{1}HNMR spectrum of compound 4b.

The synthesis of the new 5-bromoindole-2-carboxylic acid oxadiazole derivatives is presented in scheme 1.

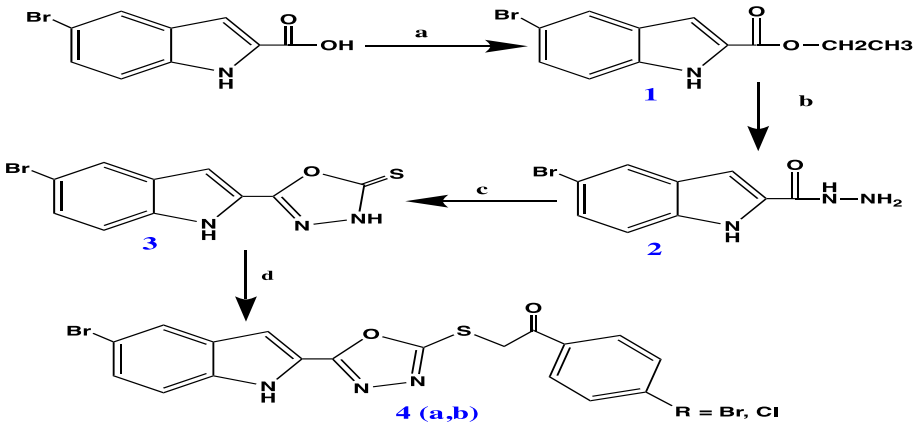

Scheme 1. Schematic diagram for the synthesis of compounds 4a and 4b. Reagents and Conditions: **a**) (**1**) EtOH, H_2SO_4 (5 ^{o}C), 80 ^{o}C, 9 h; **b**) (**2**) EtOH, $N_2H_4.H_2O$, 80 ^{o}C, 9 h; **c**) **(3)** CS_2/KOH, EtOH, 80 ^{o}C, 15 h; **d) (4a, 4b)** EtOH, TEA, 25 ^{o}C, 4h.

Molecular docking studies

Method of docking process

The molecular docking studies were performed as described previously. [15-17]

Validation of molecular docking

The molecular modeling algorithm was initially validated by redocking the co-crystallized ligand (4HJO= erlotinib) into the kinase domain of the respective receptor (EGFR), and estimating the root mean square deviation (RMSD) for the proposed docking algorithm's reliability and reproducibility. When erlotinib was docked on EGFR tyrosine kinase, the RMSD value was 1.36 Å, (below 2.00 Å), implying a proven algorithm once compared to the crystallographic structure

method for MD simulations studies

This methodology was carried out in accordance with the previously reported work. [18,19]

Results and discussion

Chemistry

The IR spectrum of compound **3** showed a band at 2642 (SH) str. of oxadiazole and 1161,1083 (C-O-C) str., while compound **4a** revealed a band at 1674 cm-1(C=O) str., 1620 cm-1(C=C) str., 1577 (C=N) str., and 1165,1064 cm^{-1} (C-O-C) str. The IR spectrum of compound **4b** revealed characteristic absorption bands at 3205 (NH) str. of indole, 1678 cm-1(C=O) str, 1589 cm-1 (C=N) str, and 1165,1091cm^{-1} (C-O-C) str. The ^{1}HNMR interpretation for compound **3** revealed a *singlet*, due to the NH-thione group at δ= 12.44 ppm. Compound **4a** showed a distinct *singlet*, due to (CH_2) at δ=5.20 ppm, and compound **4b** revealed distinct signal as *singlet,* for (CH_2) at δ= 5.21ppm.

Docking studies

Affinity scores of the new indole oxadiazole derivatives against EGFR tyrosine kinase

The computational methods, commonly referred to as "in silico" methods, are frequently used in the stages of drug design and drug discovery to assess the biological activities and predicted affinities of various types of molecules, including natural products, synthetic compounds, and semisynthetic molecules. These techniques have enhanced our knowledge of the targeted areas and the discovery of substances that function as either activators or inhibitors. In this work, computer-based methods were used to examine the potential affinities of the newly synthesized oxadiazole derivatives towards a particular site on the protein known as EGFR tyrosine kinase. The energies for the target protein and the synthesized compounds were reduced using the MMFF94 force field. The protein was initially downloaded from the PDB (Protein ID: 4HJO). The next step was molecular docking, which produced 20 poses in which the optimal orientations were chosen. A table with the RMSD values, and affinity scores (ΔG) for these orientations was created (Table 1).

Table 1. Affinity scores (ΔG, kcal/mol) of indole oxadiazole derivatives against EGFR tyrosine kinase) target site.

Ligand	RMSD value (Å)	Docking score ΔG(Kcal/mol)	Interactions	
			H.B	*pi*
Compound 3	0.66	-6.13	1	12
Compound 4a	1.20	-8.06	1	8
Compound 4b	0.56	-8.18	1	14
Erlotinib	1.06	-7.61	1	7

The binding affinity of the new indole oxadiazole derivatives to the active site of EGFR tyrosine kinase

The binding affinity of the crystal ligand (erlotinib) demonstrated an energy of interaction of -7.61 kcal/ mol against EGFR tyrosine kinase. Erlotinib formed seven *pi*-alkyl and *pi*-sigma interactions with Leu694, Leu820, Ala719, Val702 and Lys721, additionally, it formed a hydrogen bond with Met769 with a distance of 1.98 Å (Figure 7).

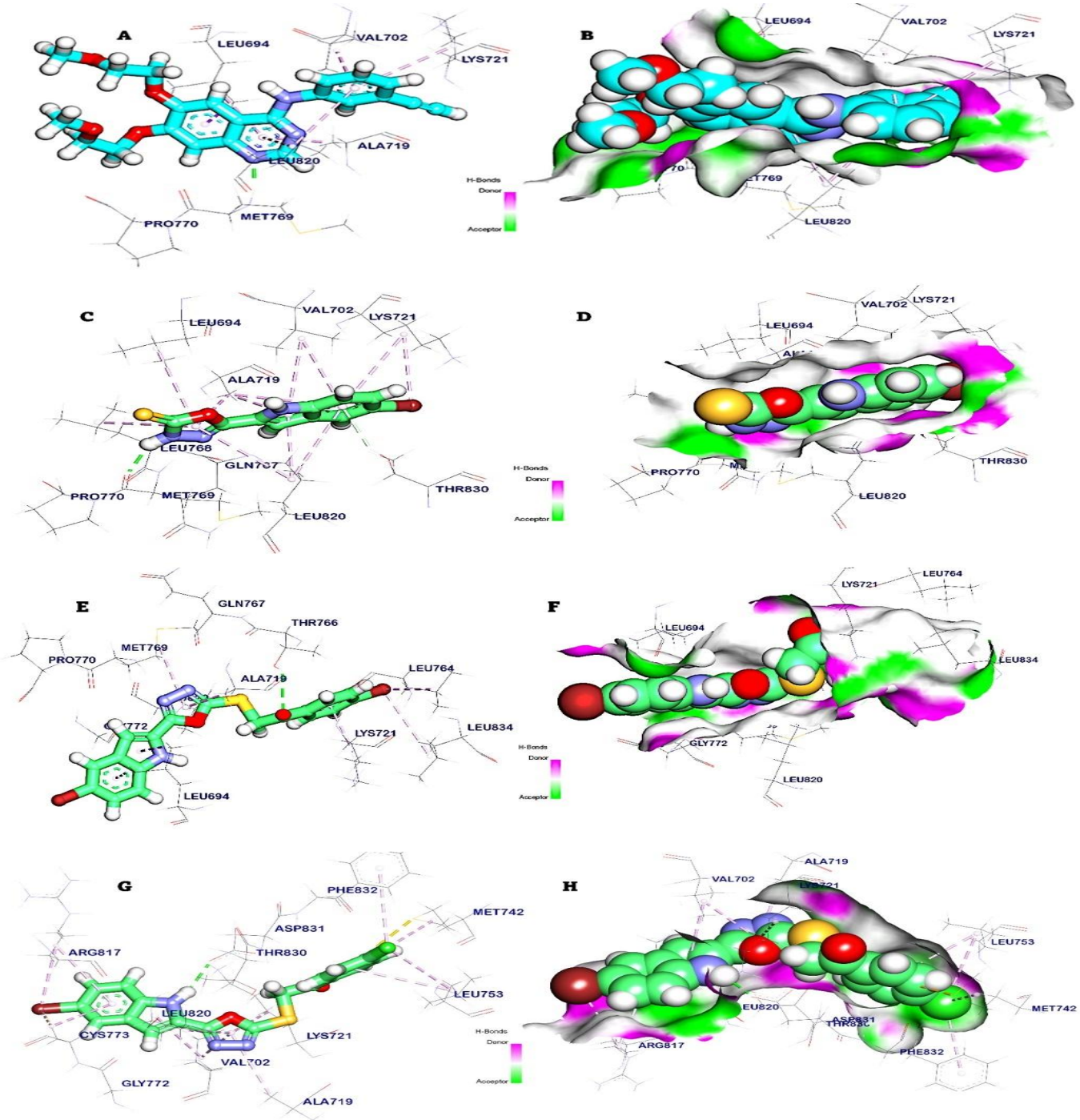

Figure 7. Molecular docking of erlotinib and compounds 3, 4a, and 4b in EGFR tyrosine kinase. (A, B): 2D and 3D mapping surface of the crystal ligand **erlotinib** docked in EGFR tyrosine kinase, (C and D): 2D and 3D mapping surface of compound **3** docked in EGFR tyrosine kinase, (E and F): 2D and 3D mapping surface of compound **4a** docked in EGFR tyrosine kinase, (G and H): 2D and 3D mapping surface of compound **4b** docked in EGFR tyrosine kinase.

Compound **3** exhibited an energy of interaction of -6.13 kcal/ mol against EGFR tyrosine kinase. Which produce twelve pi-Alkyl interactions with Leu820, Lys721, Ala719, Leu768, Leu694 and Val702, additionally, it interacted with Met769 by one hydrogen bond with bond length 2.09 Å (Figure 7 C and D). The binding mode of compound **4a** exhibited a binding energy of -8.06 kcal/ mol against EGFR tyrosine kinase. It created six *pi*-alkyl interactions with Leu764, Met769, Leu834, Lys721, Ala719, Leu820 and two *pi*-sigma interactions with Leu694, on the other hand, compound 4a formed one H-bond with Thr766 with bond length 2.09 Å (Figure 7 E and F). The binding mode of compound **4b** exhibited a binding energy of -8.18 kcal/ mol against EGFR tyrosine kinase. Compound **4b** created fourteen *pi*-alkyl and *pi*-sulfur interactions with Cys773, Arg817, Lys721, Val702, Leu753, Phe832, Ala719, Leu820 and Met742. Additionally, it formed a H-bond with Asp831 with bond length 2.32 Å Figure 7 (G and H).

ADMET studies

The Discovery studio 2019 program can be used to conduct ADMET profile analysis on synthetic compounds. This type of study involves evaluating numerous characteristics, such as the compounds' ability to pass through the blood-brain barrier and their potential to cause hepatotoxicity in animals. The compounds in question were found to have high logp values and low solubility leading to high absorption rates. Compounds **4a** and **4b** may affect the central nervous system (CNS), due to their ability to pass through the blood-brain barrier (BBB), while compound **3** is less toxic to the CNS (Figure 8 and Table 2).

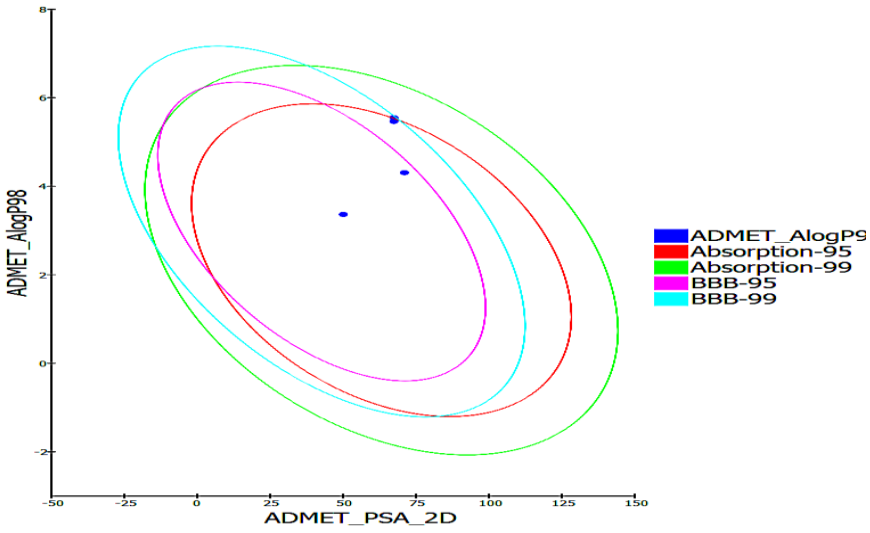

Figure 8. Predicted ADMET results for the newly synthesized compounds 3, 4a, and 4b.

Table 2. Predicted ADMET parameters for the synthesized compounds 3-4b.

Compound	BBB level	Solubility level	Absorption level[a]	Hepato-toxicity	CYP2D6 prediction[b]	PPB prediction[c]
3	Medium	Low	0	True	False	True
4a	High	Very Low	1	True	False	True
4b	High	Very Low	0	True	False	True
Erlotinib	High	Low	0	True	False	True

[a] Absorption level: 0 = good, 1 = moderate, 2 = poor, 3 = very poor.

[b] CYP2D6 (cytochrome P2D6): TRUE = inhibitor, FALSE = non inhibitor. The classification of whether a compound is a CYP2D6 inhibitor using the cutoff Bayesian score of 0.161.

[c] PBB (plasma protein binding): FALSE means less than 90%, TRUE means more than 90%.

The classification of whether a compound is highly bounded (≥90% bound) to plasma proteins using the cutoff Bayesian score of -2.209.

Density Functional Theory (DFT) Study

The electronic characteristics of the synthesized compounds **3**, **4a** and **4b** were evaluated using the Discovery Studio program. Erlotinib was used as a reference. Total energy (kcal/mol), binding energy (kcal/mol), HOMO energy (kcal/mol), LUMO energy (kcal/mol), and dipole moment were computed using density functional theory (DFT). The ligand's interactions with other species are described by the HOMO and LUMO orbitals, HOMO is associated with the ability to donate electrons, LUMO is connected to the reception of electrons. The gap energy can be used to make a rough calculation of the chemical and kinetic stability of a compound, and the total dipole moment of a molecule can characterize how well it interacts with its environment. The results of DFT studies are summarized in Table 3 and Figure 9. Compound **4a** is predicted to be the most stable compound which has total binding energy of -6536.6 kcal/mol and binding energy with hot amino acids of -7.64 kcal/mol. Additionally, it has a good dipole moment (2.90 debye). This in turn indicates the ability of compound **4a** to form hydrogen bonds compared to erlotinib.

Table 3. Motifs of the tested ligands' molecular orbitals and their spatial distribution.

Compound	Total Energy)	Binding Energy	HOMO Energy	LUMO Energy	Dipole moment (debye)	Band Gap Energy
3	-3,586.25	-4.47	-0.20	-0.10	0.696	0.10
4a	-6,536.67	-7.64	-0.19	-0.11	2.90	0.07
4b	-4,424.74	-7.66	-0.19	-0.11	1.92	0.07
Erlotinib	-1,305.67	-10.07	-0.19	-0.10	2.75	0.09

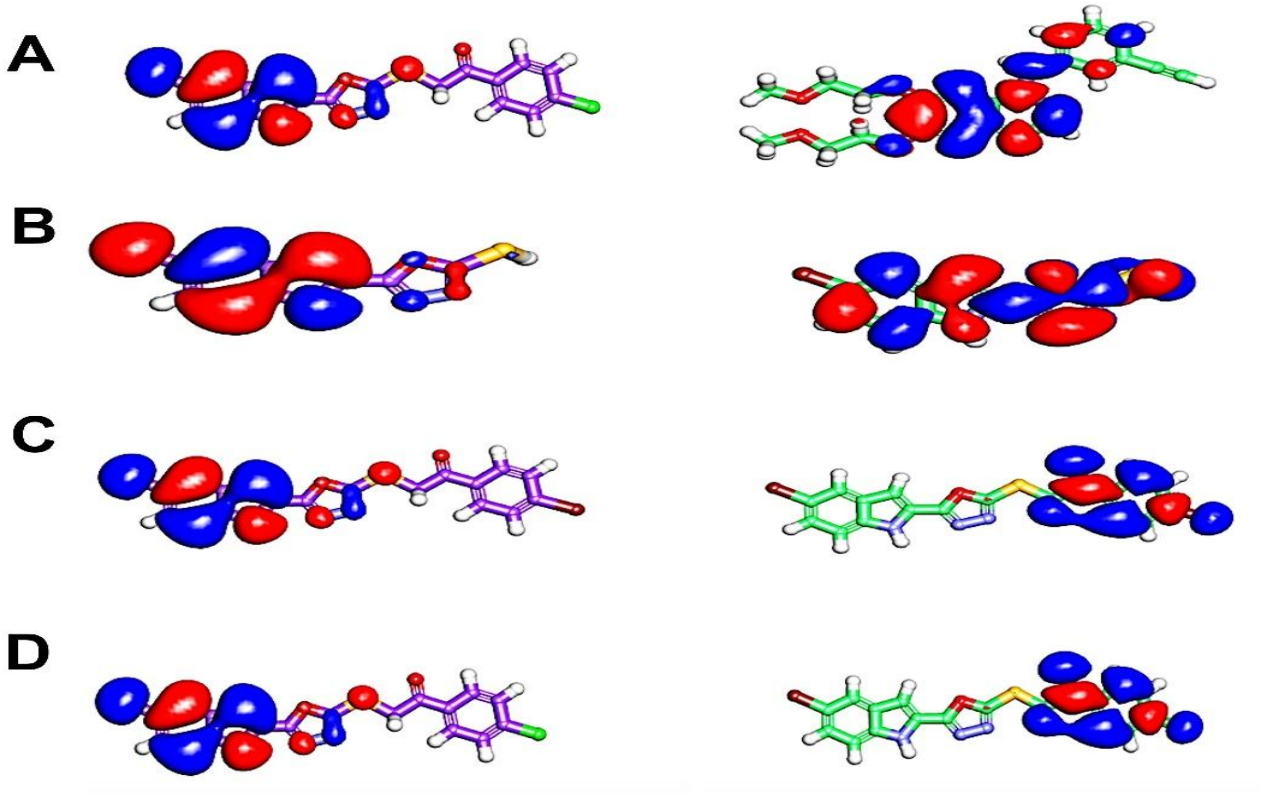

Figure 9. Three-dimensional distribution of molecular orbitals for: A. Crystal ligand Erlotinib; B. Compound 3; C. Compound 4a; and D. Compound 4b.

MD Simulations studies

RMSD was used to figure out how stable the protein-ligand complex (EGFR tyrosine kinase-compound **4a**/**4b**) was in its apo and ligand-bound states by measuring how the atoms in the backbone moved and changed shape. During the simulation, it is seen that the RMSD for the protein, ligand, and complex is lower and there weren't any big changes, which shows that they are more stable. To get a better idea of which parts of EGFR tyrosine kinase are changing during the simulation, the RMSF of each residue was

used to figure out how flexible it was. It was clear that adding a ligand (compound **4a** or compound **4b**) to EGFR tyrosine kinase didn't make any of its residues more flexible. The radius of gyration (Rg) showed how close together the complex was. The more compact a system is, the less it changes over the course of the simulation. It was found that the Rg of the complex was less than that of the starting period. During the simulation, the solvent accessible surface area (SASA) was used to measure how the protein-ligand complexes and the solvents interacted. In another word, the SASA of the complex was calculated to figure out how much its shape changed during the interaction. The protein's surface area decreased, which was interesting, and the SASA value was lower than it was at the beginning. The structure of a protein-ligand complex must be held together by hydrogen bonds. It was seen that the protein could form up to five hydrogen bonds with either compound **4a** or compound **4b** in its most stable form (Figure 10 and 11).

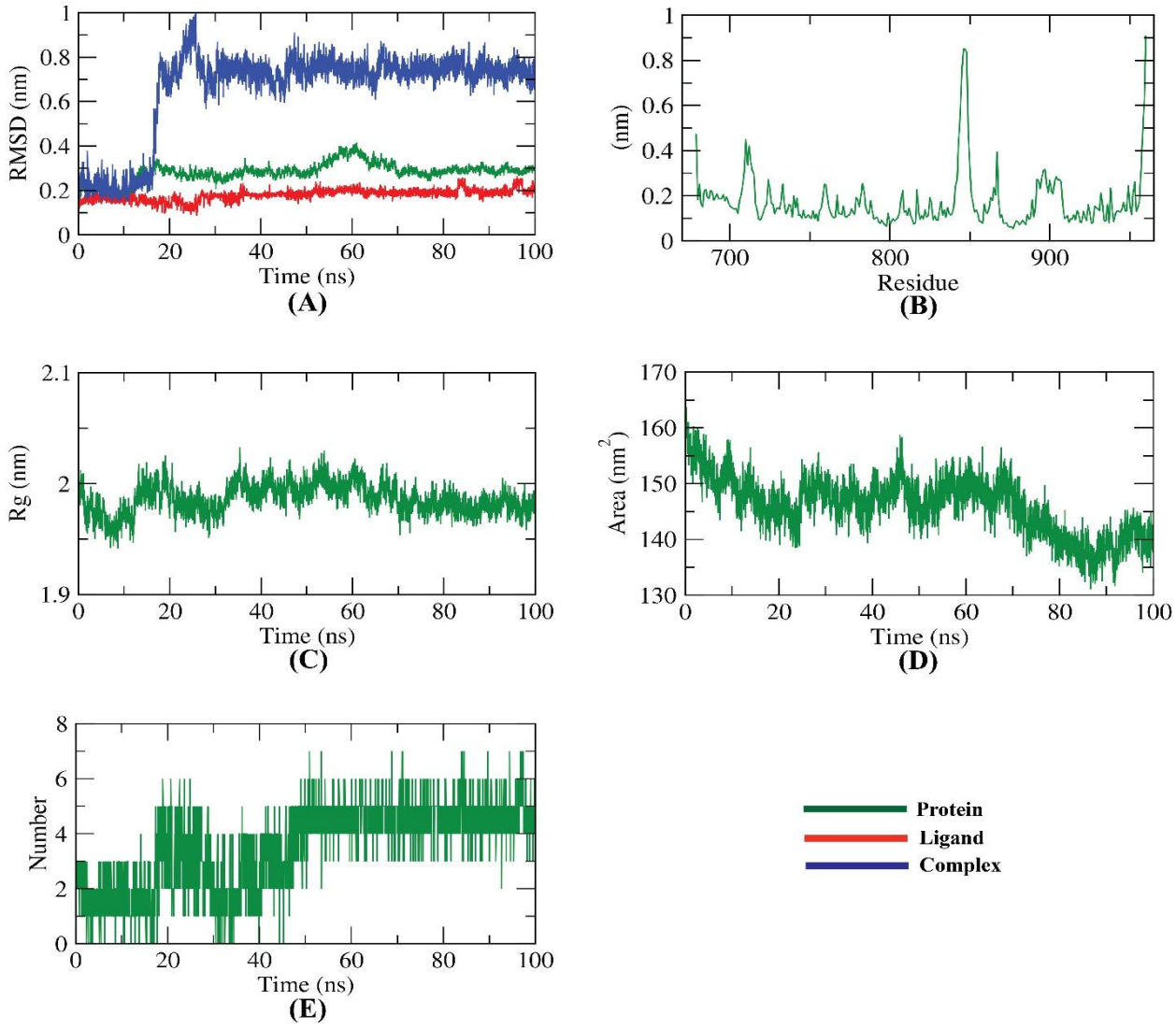

Figure 10. MD simulation results for EGFR tyrosine kinase and compound 4a.

A. RMSD values of compound **4a,** EGFR tyrosine kinase and **4a**-EGFR tyrosine kinase complex; B. RMSF; C. R_g; D. SASA of EGFR tyrosine kinase; E. H-bonding of **4a**-EGFR tyrosine kinase complex in the MD run.

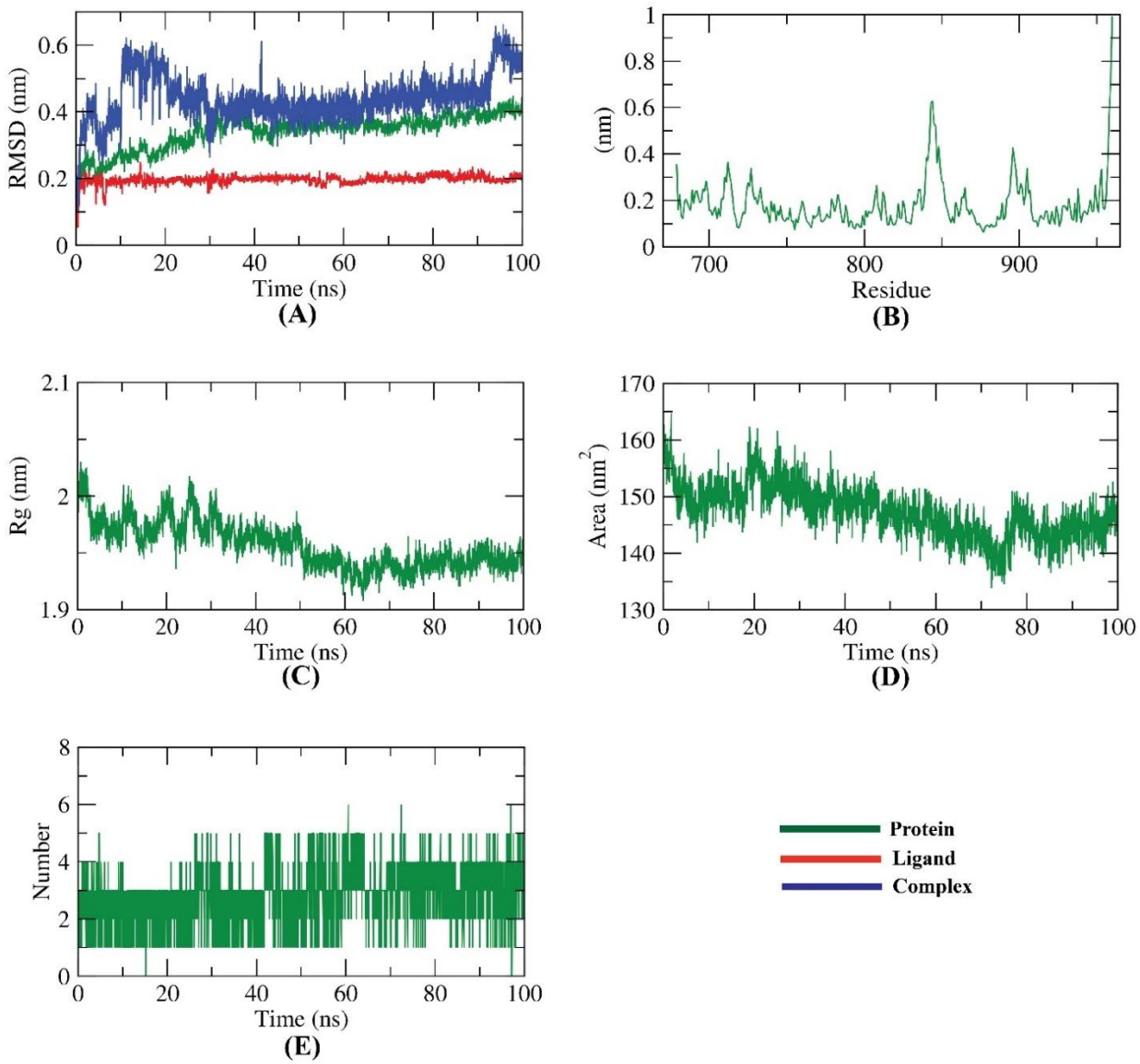

Figure 11. MD simulation results for EGFR tyrosine kinase and compound 4b.

A. RMSD values of compound **4b**, EGFR tyrosine kinase and **4b**-EGFR tyrosine kinase complex; B. RMSF; C. R_g; D. SASA of EGFR tyrosine kinase; E. H-bonding of **4b**-EGFR tyrosine kinase complex in the MD run.

Molecular Mechanics/Poisson–Boltzmann Surface Area (MM/PBSA) of compound 4a

We used the MM/PBSA method to figure out the binding free energy of the EGFR tyrosine kinase-compound **4a** complex for

the last 20 ns of the MD production run, with a 100 ps time step. We also used the MmPbSaStat.py script, which took the output files from g mmpbsa and used them to figure out the average free binding energy and its standard deviation/error. The ligand had -116 KJ/mol of free energy when it was bound to the protein. Also, we found out how much binding free energy each protein residue added to the interaction between the protein and the ligand. The contribution of each residue was worked out by breaking down the total binding free energy of the system into the energy contributed by each residue. This helped us figure out which residues are "crucial" for binding of compound **4a** to EGFR tyrosine kinase. It was found that the protein residues Leu753, Leu764, Leu768, Leu820, and Leu837 all contributed more than -4 KJ/mol of binding energy. This means that they are "hotspot" residues that help the ligand bind to the protein (Figure 12).

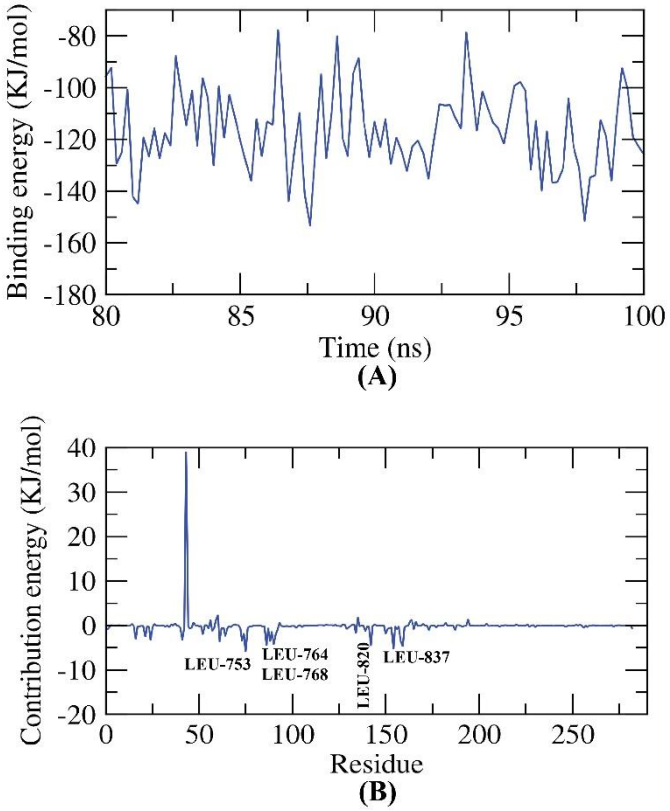

Figure 12. Plot of MM/PBSA binding free energy contribution per residue of compound **4a**-EGFR tyrosine kinase complex.

Molecular Mechanics/Poisson–Boltzmann Surface Area (MM/PBSA) of compound 4b

Using the MM/PBSA approach, we analysed MD trajectories and determined the binding free energy of the protein-ligand complex (EGFR tyrosine kinase-compound **4b** complex) over the final 20 ns of the production run, with a 100 ps time step. The binding free energy of the

ligand to the protein was -123 KJ/mol. Furthermore, we calculated the binding free energy contribution of each protein residue to the total. Each residue's contribution was determined by detailed analysis of the system's total binding free energy into its component parts. As a result, we were able to identify the "critical" residues that have a positive role in the binding of this chemical to the protein. Hotspot residues involved in ligand binding were identified as Val702, Leu753, Thr766, and Leu820 (Figure 13).

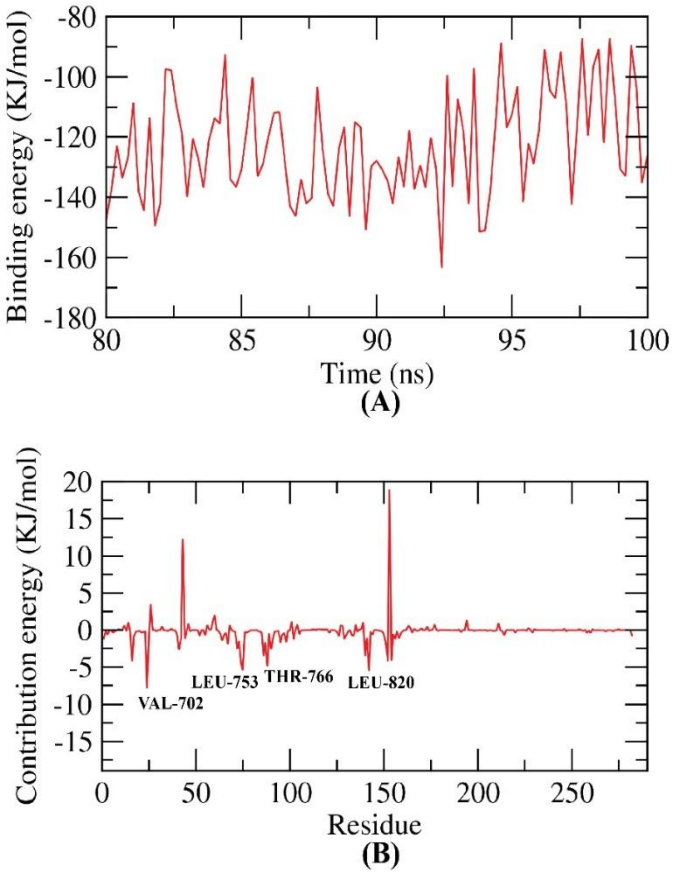

Figure 13. Plot of MM/PBSA binding free energy contribution per residue of compound **4b**-EGFR tyrosine kinase complex.

Conclusion

In conclusion, 5-bromoindole-2-carboxylic acid was effectively used to produce two new indole oxadiazole derivatives (compounds **4a** and **4b**). Various physical (color, melting point) and spectroscopic analyses were used to identify and describe the newly synthesized chemicals (FT-IR, ^{1}HNMR). The derivatives were shown to have an excellent pharmacokinetic profile, and DFT studies showed that compound **4a** is the most stable compound. Furthermore, compound **4a** was shown to have a good dipole moment (2.90 debye), which indicates the ability of compound **4a** to

form hydrogen bonds compared to erlotinib. MD simulation showed that EGFR tyrosine kinase could form up to five hydrogen bonds with compound **4a** in its most stable form. Finally, Molecular Mechanics/Poisson–Boltzmann Surface Area showed that compound **4a** developed "hotspot" residues that help it bind to EGFR tyrosine kinase.

Acknowledgement

The authors sincerely appreciate the help provided by the Department of Pharmaceutical Chemistry, College of Pharmacy, University of Baghdad.

Conflict of Interest

The authors report no potential conflict of interest.

References

1. Dhatchinamoorthy K, Colbert JD, Rock KL. Cancer immune evasion through loss of MHC class I antigen presentation. *Frontiers in immunology*. 2021; 12: 636568.

2. Brenner H. Long-term survival rates of cancer patients achieved by the end of the 20th century: a period analysis. *The Lancet*. 2002; 360(9340): 1131-5.

3. Ivan BC, Barbuceanu SF, Hotnog CM, Anghel AI, Ancuceanu RV, Mihaila MA, Brasoveanu LI, Shova S, Draghici C, Olaru OT, Nitulescu GM. New pyrrole derivatives as promising biological Agents: Design, synthesis, characterization, in silico, and cytotoxicity evaluation. *International Journal of Molecular Sciences*. 2022; 23(16): 8854.

4. Umer SM, Solangi M, Khan KM, Saleem RS. Indole-containing natural products 2019–2022: Isolations, reappraisals, syntheses, and biological activities. *Molecules*. 2022; 27(21): 7586.

5. Ogiso H, Ishitani R, Nureki O, Fukai S, Yamanaka M, Kim JH, Saito K, Sakamoto A, Inoue M, Shirouzu M, Yokoyama S. Crystal structure of the complex of human epidermal growth factor and receptor extracellular domains. *Cell*. 2002; 110(6): 775-87.

6. Wee P, Wang Z. Epidermal growth factor receptor cell proliferation signaling pathways. *Cancers*. 2017; 9(5):52.

7. Katz M, Amit I, Yarden Y. Regulation of MAPKs by growth factors and receptor tyrosine kinases. *Biochimica et Biophysica Acta (BBA)-Molecular Cell Research*. 2007; 1773(8): 1161-76.

8. Thomas R, Weihua Z. Rethink of EGFR in cancer with its kinase independent function on board. *Frontiers in Oncology*. 2019; 9:800.

9. Konieczkowski DJ, Johannessen CM, Garraway LA. A convergence-based framework for cancer drug resistance. *Cancer cell*. 2018; 33(5): 801-15.

10. Martins P, Jesus J, Santos S, Raposo LR, Roma-Rodrigues C, Baptista PV, Fernandes AR. Heterocyclic anticancer compounds: recent advances and the paradigm shift towards the use of nanomedicine's tool box. *Molecules*. 2015; 20(9):16852-91.

11. Desai N, Monapara J, Jethawa A, Khedkar V, Shingate B. Oxadiazole: A highly versatile scaffold in drug discovery. *Archiv der Pharmazie*. 2022: e2200123.

12. Hassan OM, Sarsam SW. Synthesis, characterization and preliminary anti-inflammatory evaluation of new etodolac derivatives. *Iraqi Journal of Pharmaceutical Sciences* (P-ISSN: 1683-3597, E-ISSN: 2521-3512). 2019; 28(1): 106-12.

13. Yaseen Y, Kubba A, Shihab W, Tahtamouni L. Synthesis, docking study, and structure-activity relationship of novel niflumic acid derivatives acting as anticancer agents by inhibiting VEGFR or EGFR tyrosine kinase activities. *Pharmacia*. 2022; 69(3):595-614.

14. Ajani OO, Iyaye KT. Recent advances on oxadiazole motifs: Synthesis, reactions and biological activities. *Mediterr . J. Chem*. 2020;10:418-52.

15. Abbas AH, Mahmood AA, Tahtamouni LH, Al-Mazaydeh ZA, Rammaha MS, Alsoubani F, Al-bayati RI. A novel derivative of picolinic acid induces endoplasmic reticulum stress-mediated apoptosis in human non-small cell lung cancer cells: synthesis, docking study, and anticancer activity. *Pharmacia*. 2021; 68(3):679-92.

16. Hassan OM, Razzak Mahmood AA, Hamzah AH, Tahtamouni LH. Design, synthesis, and molecular docking studies of 5-Bromoindole-2-carboxylic acid hydrazone derivatives: In vitro anticancer and VEGFR-2 inhibitory effects. *Chemistry Select*. 2022; 7(46) : e202203726.

17. Abbas AH, Mahmood AA, Tahtamouni LH, Al-Mazaydeh ZA, Rammaha MS, Alsoubani F, Al-bayati RI. A novel derivative of picolinic acid induces endoplasmic reticulum stress-mediated apoptosis in human non-small cell lung cancer cells: synthesis, docking study, and anticancer activity. *Pharmacia*. 2021; 68:679.

18. Kubba AA, Rahim NA. Synthesis, characterization and antimicrobial evaluation with DFT study of new two-amino-4-(4-chlorophenyl) thiazole derivatives. *Iraqi Journal of Pharmaceutical Sciences* (P-ISSN:

1683-3597, E-ISSN: 2521-3512). 2018; 27(1): 79-88.

19. Abbas SS, Kubba AA. Synthesis and antimicrobial evaluation with DFT study for new thiazole derivatives. *Iraqi Journal of Pharmaceutical Sciences* (P-ISSN: 1683-3597, E-ISSN: 2521-3512). 2018; 27(1):69-78.